energies

MDPI

Article

Experimental Investigation of the Combustion Characteristics of Briquettes Produced from Sawdust and Coal in a Fixed-Bed Reactor

John Mbũrũ Ngũgĩ *, Solomzi Marco Ngalonkulu and Zhongjie Huan

Department of Mechanical and Mechatronics Engineering, Tshwane University of Technology, Staatsartillerie Rd, Pretoria West, Pretoria 0183, South Africa; ngalonkulus@tut.ac.za (S.M.N.); huanz@tut.ac.za (Z.H.)
* Correspondence: ngugijm@tut.ac.za or ngugijohnmburu@outlook.com

Abstract

The utilization of biomass-coal briquettes offers a promising approach for improving the sustainability and performance of solid-fuel combustion systems. This study experimentally investigated the combustion characteristics of sawdust-coal briquettes in a fixed-bed reactor to evaluate the influence of fuel composition on combustion behavior. Briquettes containing 0–60 wt.% coal at 10 wt.% intervals were produced and combusted under a constant air mass flux of 0.10 kg/m^{2}s. Combustion performance was assessed using temperature distribution, mass-loss history, ignition time, flame propagation speed, and burning rate. Temperature profiles exhibited a single dominant peak, indicating substantial overlap of fuel heating, devolatilization, volatile combustion, and char oxidation processes. Peak bed temperatures decreased from 813 °C for briquettes containing 40 wt.% sawdust to 657 °C for pure sawdust briquettes, while combustion duration decreased from 26 to 21 min with increasing sawdust content. Mass-loss rate, flame propagation speed, and burning rate increased with increasing sawdust content, while ignition time decreased progressively. Overall, higher sawdust contents promoted earlier ignition, faster fuel conversion, and greater combustion reactivity, whereas higher coal contents resulted in elevated combustion temperatures and longer combustion durations. These findings provide insights for optimizing biomass-coal briquette formulations for fixed-bed combustion applications.

Keywords: briquettes; fixed-bed combustion; ignition time; flame propagation speed; burning rate

1. Introduction

The rising global energy demand, coupled with concerns over fossil fuel depletion and environmental harm, has intensified efforts to identify sustainable alternatives [1]. Biomass stands out as a renewable option due to its abundance, carbon-neutral profile, and potential to partially replace fossil fuels while lowering greenhouse gas emissions [2,3]. Sawdust, a key by-product of wood-processing, represents a valuable biomass resource whose utilization can simultaneously reduce waste and support sustainable energy generation [1,4]. When processed into briquettes, pellets, or biochar, it offers cleaner-burning substitutes for coal, delivering environmental benefits despite lower calorific values, while also stabilizing carbon and advancing circular economy practices [1].

Coal remains a major energy source worldwide due to its high calorific value, abundant reserves, and well-established conversion and utilization technologies [5–7]. Nevertheless, coal combustion is a significant contributor to environmental pollution, releasing large

Check for updates

Received: 7 September 2026
Revised: 5 October 2026
Accepted: 8 October 2026
Published: 29 October 2026

Copyright: © 2026 by the authors. Licensee MDPI, Basel, Switzerland. This article is an open access article distributed under the terms and conditions of the Creative Commons Attribution (CC BY) license.

quantities of carbon dioxide (CO_2), sulfur oxides (SO_x), nitrogen oxides (NO_x), particulate matter (PM), and polycyclic aromatic hydrocarbons (PAHs) [8,9]. These emissions adversely affect air quality, contribute to climate change, and pose serious risks to human health [10,11]. As a result, the co-utilization of biomass with coal has gained substantial research attention as a promising strategy to reduce greenhouse gas emissions and other harmful pollutants while maintaining the reliability, energy security, and operational flexibility of existing coal-based energy systems [12–16].

The thermochemical co-processing of coal and biomass has attracted considerable attention as a strategy for improving fuel sustainability while reducing the environmental impacts of coal utilization [12–14]. Previous research has focused on co-combustion, co-gasification, and co-pyrolysis, with studies demonstrating that biomass addition enhances fuel reactivity because of its high volatile matter content, oxygen-rich structure, and higher H/C ratio. These properties promote ignition and facilitate the thermal decomposition of coal during conversion [12,13].

Co-pyrolysis studies of sawdust-coal blends using thermogravimetric analysis (TGA) and fixed-bed reactors have reported positive synergistic effects, including enhanced volatile release, reduced char yields, increased gas production, and improved gas calorific value compared with additive predictions [13]. Park et al. [13] reported maximum synergy at approximately 600 °C and a sawdust blending ratio of 0.6, attributing the effect to hydrogen transfer from the biomass and the catalytic activity of biomass-derived inorganic species. Furthermore, co-combustion studies have shown that biomass generally lowers ignition temperatures and increases combustion reactivity, although the extent of synergy depends on biomass type, composition, and operating conditions [11,12].

Despite these advances, most investigations have focused on pulverized fuels or loose biomass-coal mixtures under TGA, combustion, or pyrolysis conditions [12–14,17]. Comparatively little attention has been devoted to densified biomass-coal fuels such as briquettes. Briquetting alters important fuel characteristics, including density, porosity, particle arrangement, and heat and mass transfer properties, which can significantly affect combustion behavior [18,19]. Consequently, the performance of loose fuel blends cannot be directly extrapolated to briquetted fuels.

Fixed-bed combustion involves a sequence of coupled processes, including drying, devolatilization, volatile combustion, char oxidation, heat transfer, and oxygen transport. Performance is commonly evaluated using parameters such as ignition time, flame-front propagation rate, burning rate, reaction-zone development, combustion duration, and temperature evolution [20–23]. These parameters are important for assessing fuel behavior, combustion performance, and the suitability of briquettes for practical fixed-bed combustion systems. Although the thermal degradation, combustion kinetics, and co-pyrolysis behavior of coal–biomass blends have been widely investigated, the combustion behavior of densified sawdust–coal briquettes under fixed-bed conditions remains comparatively less understood. Further investigation is required to establish how fuel composition influences the coupled thermal and fuel-conversion processes occurring within a fixed bed.

Previous studies have largely focused on pyrolysis mechanisms, kinetic parameters, activation energies, and gaseous-product evolution, providing comparatively limited information on the integrated combustion performance of densified sawdust–coal briquettes. Therefore, systematic experimental characterization of temperature evolution, ignition behavior, combustion-front propagation, mass loss, and burning rate is needed to better understand the combustion behavior of these fuels under fixed-bed conditions.

Accordingly, this study systematically investigates the influence of sawdust–coal composition on ignition behavior, temperature evolution, flame-front propagation, mass loss, and specific burning rate in a fixed-bed reactor. By examining these combustion parameters collectively, the study seeks to establish the relationship between briquette composition and overall combustion behavior and to provide practical information for selecting and designing

sawdust–coal briquettes for fixed-bed applications. Such information can support the formulation of briquettes according to specific operational requirements, including applications where controlled heat release, sustained combustion, or rapid fuel conversion is desired.

2. Methodology

2.1. Briquette Production

Sawdust from cedar wood (*Juniperus procera*), commonly known as East African cedar or Kenya cedar, and bituminous coal were used as the raw materials for briquette production. The cedar sawdust was obtained from local sawmills in Nyeri Town, Kenya, while the bituminous coal was sourced from the Nairobi Industrial Area. Both materials were ground and sieved through a 600 µm mesh sieve to obtain a uniform particle size distribution. The sieved sawdust and bituminous coal were thoroughly mixed at prescribed mass ratios to prepare seven formulations containing 0–60 wt.% coal in 10% increments. Briquettes were produced using a cylindrical steel mold and plunger assembly. The mold had an internal diameter of 25 mm and a length of 100 mm, while the plunger had a matching diameter of 25 mm. A measured quantity of the prepared feedstock was loaded into the mold and compacted using a compression machine (Tecnotest, Modena, Italy); see Figure 1. The required quantities of sawdust and coal were thoroughly mixed according to the prescribed blend ratios and compressed under a constant load of 200 kN for 20 s. This arrangement produced briquettes approximately 40 mm in length. No binder was added during briquette production. The same compaction conditions were applied to all formulations to maintain consistency in the preparation procedure. However, variations in sawdust–coal composition may result in differences in the internal packing structure and density of the resulting briquettes, which may subsequently influence their combustion behavior. The compacted briquettes were subsequently extruded using a second mold with an internal diameter of 27 mm, producing briquettes of uniform size and shape. Finally, the briquettes were removed from the mold and dried under direct sunlight for several days to reduce their moisture content and enhance their mechanical strength. The dried briquettes were then stored in sealed containers to prevent moisture reabsorption prior to combustion testing in the fixed-bed reactor.

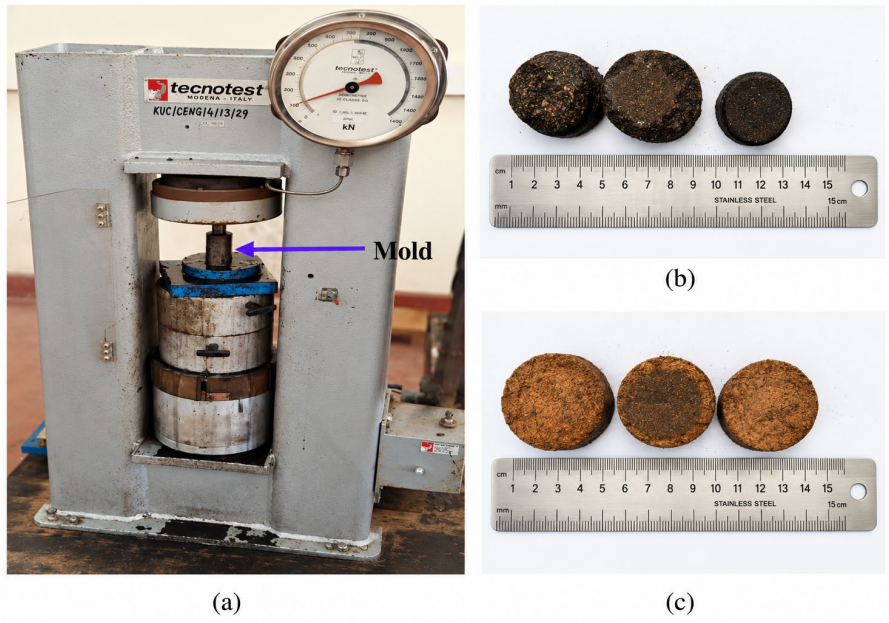


Figure 1. Experimental setup and briquette samples: (**a**) universal compression testing machine used for briquette compression testing together with the mold; (**b**) briquette produced from 100 wt.% coal sawdust; and (**c**) briquette produced from 100 wt.% sawdust.

2.2. Fuel Properties of Raw Materials

Proximate and ultimate analyses were conducted on the raw coal and sawdust feedstocks before briquette production to determine their fuel and chemical characteristics. These data provide the basis for interpreting briquette combustion behavior, including ignition, volatile release, char oxidation, and heat generation, and establish a baseline for evaluating the effects of coal–sawdust blending ratios on ignition time, flame-front propagation, specific burning rate, and peak bed temperature.

Briquetting primarily alters physical properties such as density, particle contact, porosity, permeability, and oxygen accessibility, while the chemical composition of the briquettes remains dependent on the parent fuels. Therefore, the proximate and ultimate properties of the feedstocks were used as the compositional reference for interpreting briquette combustion behavior, with briquetting effects considered through changes in physical structure and combustion performance. The analyses were conducted according to the procedures and standards reported by Tanui et al. [21] and Kipngetich et al. [20], and the compositions of the raw coal and sawdust are presented in Table 1.

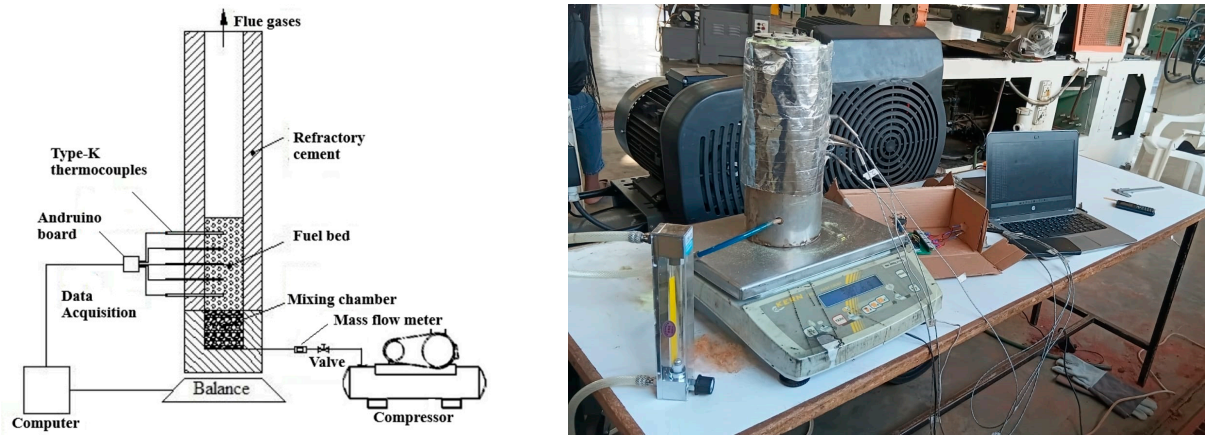
Table 1. Proximate and ultimate composition of sawdust and coal (as-received basis).

Parameter	Sawdust	Coal
Proximate analysis		
Moisture (%)	5.70	4.08
Volatile matter, VM (%)	81.02	54.81
Fixed carbon, FC (%)	11.86	38.39
Ash (%)	1.43	2.73
Total (%)	**100.01**	**100.01**
HHV (MJ/kg)	**16.51**	**21.80**
Ultimate analysis		
Carbon, C (%)	44.42	49.38
Hydrogen, H (%)	5.64	5.39
Oxygen, O (%)	42.17	37.76
Nitrogen + Sulfur, N + S (%)	0.64	0.65
Ash (%)	1.43	2.73
Moisture (%)	5.70	4.08
Total (%)	**100.00**	**100.00**

2.3. Experimental Set

All experiments were conducted using the laboratory-scale fixed-bed reactor system shown in Figure 2. The setup comprised five main components: (i) the fixed-bed reactor, (ii) a temperature data acquisition system, (iii) a fuel mass measurement unit, (iv) an airflow measurement system, and (v) an air compressor.

The reactor consisted of a vertical cylindrical combustion chamber with an internal diameter of 100 mm, an external diameter of 180 mm, and a height of 200 mm. Four thermocouple (TC1-TC4) ports were positioned along the reactor wall at 20 mm intervals to monitor temperature development within the fuel bed, with TC1 located nearest the top of the reactor and TC4 nearest the bottom. The reactor walls were fabricated from stainless steel and separated by a 40 mm thick refractory cement layer with a thermal conductivity of 0.34 W/mK [24,25]. To further reduce heat losses, the outer surface of the reactor was insulated with an 18 mm thick aluminum silicate fiber layer, which has a thermal conductivity of approximately 0.055 W/m K below 400 K [24,25].



(**a**) Schematic diagram (**b**) Photo of the laboratory setup

Figure 2. Experimental Setup and Configuration.

The reactor was operated in a counter-current combustion mode. Briquettes placed within the reactor were ignited at the top using a methane flame, after which the combustion front propagated downward through the stationary fuel bed. Atmospheric air, supplied by an air compressor at room temperature (298 K), entered the reactor through a stainless-steel perforated grate located beneath the fuel bed. The grate ensured uniform air distribution during combustion. The airflow was measured and controlled using a glass rotameter flow meter (Model LZB-25; Shanghai Automation Instrumentation Co., Ltd., Shanghai, China) with a measurement range of 1–25 m^3/h and an accuracy of ± 0.2 m^3/h, enabling precise regulation of the air supplied to the combustion process.

Fuel mass loss was determined from continuous measurements of reactor weight during combustion. The empty reactor was first weighed, then weighed again after loading the briquettes to determine the initial fuel mass. During each experiment, the reactor was placed on a precision balance (Model FKB 16K0.1, Kern & Sohn GmbH, Balingen, Germany), with an accuracy of ± 0.1 g, and the reactor mass was recorded at one-minute intervals from ignition until complete burnout.

Temperature measurements were obtained using Type K thermocouples (Model WRNK-191; Shanghai Weilian Electronic Technology Co., Ltd., Shanghai, China) connected to thermocouple-to-digital converter modules (Model MAX31850K; Analog Devices, Inc., Wilmington, MA, USA). The modules provide a temperature resolution of 0.25 °C. Temperature data were continuously logged using an Arduino-based acquisition system and transmitted to a computer via USB for storage and subsequent analysis. Depending on operating temperature, thermocouple measurement uncertainty ranged from ± 2.184 °C to $\pm$ 6.630 °C.

To maintain consistent operating conditions, all experiments were conducted at a fixed air mass flux of 0.10 kg/m^2s. Seven briquette formulations were evaluated, with coal content ranging from 0 to 60 wt.% in 10 wt.% increments. This provided a common nominal air-supply condition for comparing the combustion characteristics of the different formulations. However, variations in sawdust–coal composition may result in different theoretical oxygen requirements. Therefore, maintaining a constant air mass flux ensured a comparable inlet air supply per unit reactor cross-sectional area but did not necessarily establish equivalent stoichiometric conditions for all formulations. Consequently, the observed differences in combustion characteristics reflect the response of the different fuel compositions under the specified air-supply condition, rather than fuel composition alone under equivalent stoichiometric conditions.

2.4. Determination of Combustion Parameters

2.4.1. Temperature Distribution in the Fixed Bed Reactor

Temperature distribution within the fuel bed was determined from temperature data recorded by the four Type-K thermocouples installed at different axial locations in the reactor (Figure 2). Measurements were collected at 60 s intervals throughout each combustion experiment.

The recorded data were used to construct temperature-time profiles for each thermocouple position, allowing for evaluation of the spatial and temporal evolution of the combustion process. As the combustion front advanced through the fuel bed, the temperature at each location increased, reached a maximum value, and then declined after the reaction zone passed.

Peak temperatures measured at different thermocouple locations were used to characterize the axial temperature distribution within the reactor. In addition, the time difference between successive peak temperatures was used to track combustion-front movement and determine the flame propagation rate through the fixed bed.

2.4.2. Mass Loss History

Mass-loss history was determined by continuously recording the mass of the entire reactor using an electronic weighing balance throughout combustion. Combustion was considered complete when the mass stabilized and the fuel-bed temperature declined substantially, indicating that significant fuel conversion had largely ceased. Flue gases exited freely without connection to an exhaust duct, avoiding forces transmitted through an exhaust connection. The relatively low air mass flux of 0.10 kg/m^{2}s was expected to limit the momentum of escaping gases; therefore, their aerodynamic forces on the reactor supported by the balance were treated as minimal. Thermal insulation and separation reduced heat transfer to the balance and minimized thermal disturbances, including surrounding-air density changes that could affect the apparent weight of the reactor assembly. However, aerodynamic and buoyancy effects were not independently quantified, and residual influences cannot be entirely excluded. The recorded mass-loss histories were used to characterize the temporal progression of fuel consumption.

2.4.3. Flame Front Propagation Speed

The flame propagation speed (V_F) was estimated from temperature measurements recorded at successive thermocouple locations along the fuel bed. It was calculated by dividing the distance between adjacent thermocouples (Δx) by the time interval (Δt) between their corresponding peak-temperature responses, as given by Equation (1) [20]:

$$V_F = \frac{\Delta x}{\Delta t} \quad (1)$$

Peak temperature was used as a consistent reference for comparing the progression of the combustion front across briquette compositions, as the distinct temperature maxima provided identifiable points for tracking the thermal response along the fuel bed. The resulting velocity represents an apparent flame propagation speed based on the progression of temperature peaks. The standard deviation of the three successive segment-specific speeds was used to indicate spatial variability along the measurement zone.

2.4.4. Ignition Time

Ignition time (t_{ig}) was determined from the temperature–time history recorded by thermocouple T_1, which was located closest to the ignition region. The first recorded T1 temperature was taken as the baseline temperature. The temperature-rise rate (dT/dt)

was calculated from the recorded temperature data to identify the initial sustained rapid-temperature-rise region associated with ignition. A tangent was fitted to this rapid-rise region and extrapolated to its intersection with the initial baseline temperature, as illustrated in Figure 3. The time corresponding to this intersection was defined as the ignition time. The same baseline definition and slope-based tangent-intersection procedure were applied consistently to all briquette formulations. Ignition behavior was influenced by fuel properties, including particle size, as well as air-mass flux, all of which affect heat transfer and volatile release during combustion.

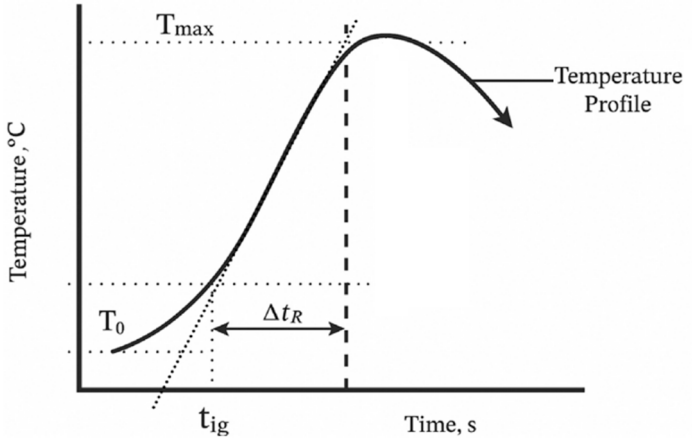


Figure 3. Determination of ignition time from temperature profiles.

2.4.5. Burning Rate

The burning rate (BR) quantifies the rate of fuel consumption during combustion and is widely used as an indicator of biomass combustion intensity. It is defined as the mass of fuel consumed per unit cross-sectional area of the fuel bed and per unit time, allowing comparisons across experiments with different bed dimensions and fuel loadings [26,27].

Combustion is considered complete when mass loss ceases and the fuel-bed temperature decreases significantly. The average burning rate for the entire combustion process was calculated using Equation (2):

$$BR = \frac{\Delta m}{A\Delta t} \quad (2)$$

where BR is the burning rate (kg/m^2s), Δm is the total mass of fuel consumed (kg), A is the fuel-bed cross-sectional area (m^2), and Δt is the combustion duration (s). A higher burning rate indicates faster fuel consumption, greater combustion intensity, increased heat release, and more rapid flame propagation through the fuel bed. Consequently, burning rate is an important parameter for assessing combustion performance, fuel reactivity, and the effects of operating conditions on biomass fuel-bed combustion.

2.4.6. Regression Analysis

Regression analysis was employed to investigate the relationship between briquette composition and combustion characteristics, namely ignition time, flame propagation speed, and specific burning rate. Sawdust content (%) was used as the independent variable, while each combustion parameter was treated as a dependent variable. Linear regression was applied to quantify the direction and magnitude of the observed relationships. The coefficient of determination (R^2) was used to evaluate the goodness of fit of the regression models. The fitted equations and regression coefficients were used to describe how variations in sawdust–coal composition were associated with changes in the measured combustion characteristics. The regression results were interpreted to identify trends in ignition time, flame

propagation speed, and specific burning rate across the investigated briquette compositions under the experimental conditions.

3. Results and Discussion

3.1. Temperature Distribution and Peak Bed Temperature

Figure 4 illustrates the temperature distribution within the combustion bed for briquettes containing different proportions of sawdust and coal. For all compositions, Thermocouple (TC1) generally reached its maximum temperature before TC2, TC3, and TC4, indicating the downward propagation of the combustion front through the fuel bed. The delay in peak temperature occurrence between successive thermocouples confirms progressive heat transfer from the ignition zone to adjacent fuel layers and the gradual movement of the flame front.

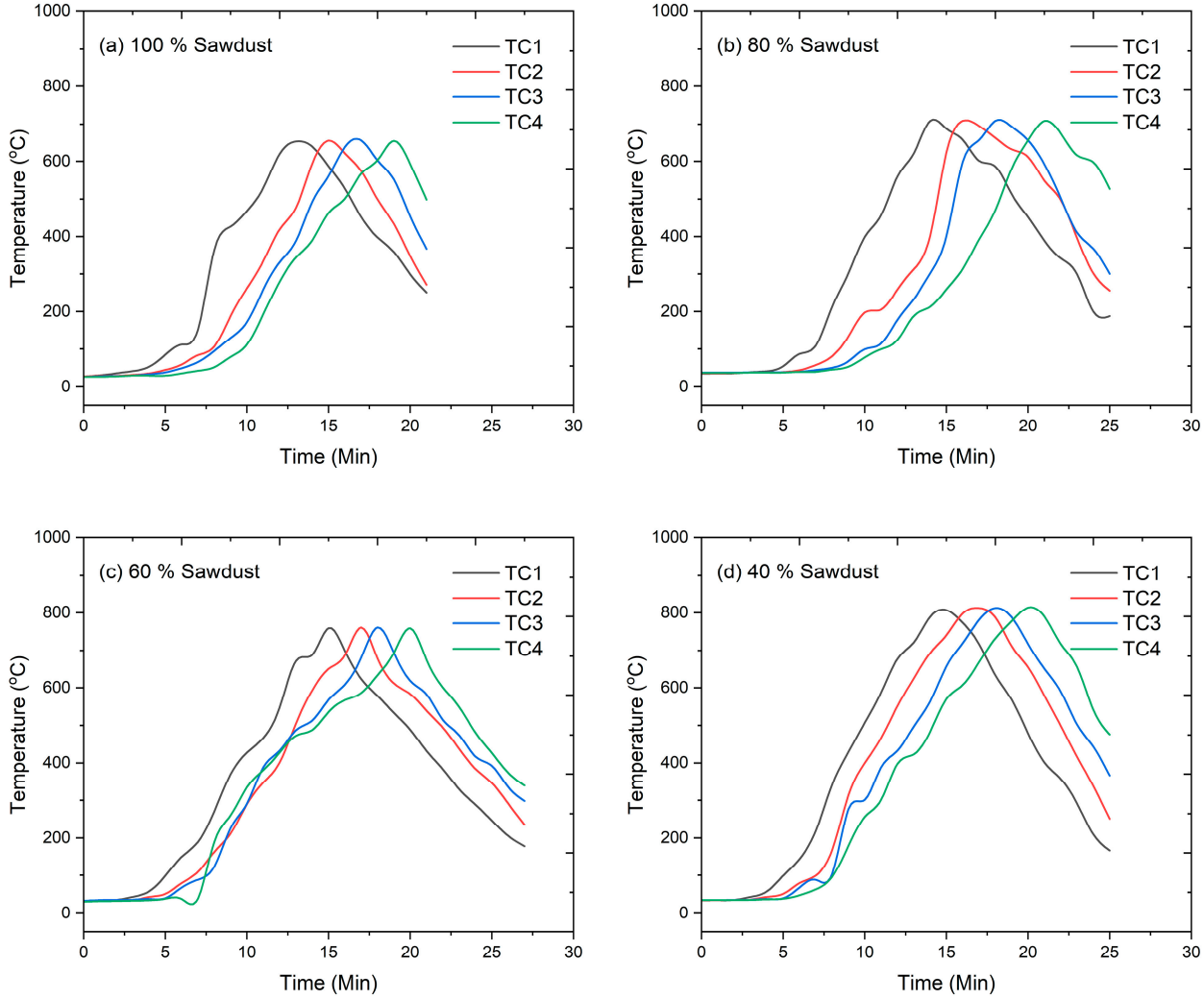


Figure 4. Temperature evolution at different bed locations (TC1-TC4) during fixed-bed combustion of briquettes prepared with different sawdust-coal blending ratios.

For all briquette compositions, the temperature increased gradually, rose rapidly to a peak, and subsequently declined. This behavior is characteristic of fixed-bed combustion and reflects the combined thermal effects of fuel heating, drying, devolatilization, volatile combustion, char oxidation, and burnout. The presence of a single temperature peak at each thermocouple may suggest an overlap in the thermal effects of these processes within the measured temperature profiles. However, temperature measurements alone cannot establish

whether the individual processes occur simultaneously or sequentially. During combustion, heat released by oxidation reactions is partly consumed by moisture evaporation and endothermic fuel-conversion processes, while the remaining energy contributes to the increase in bed temperature. Consequently, the observed temperature profiles reflect the net balance between heat generation, heat consumption, and heat transfer within the fuel bed.

Although the temperature profiles exhibited similar shapes, the peak temperatures varied considerably with fuel composition. Figure 5 shows that the experimental peak bed temperature decreased from approximately 813 °C at 40% sawdust to 657 °C at 100% sawdust, representing a reduction of about 19%. Regression analysis confirmed a strong inverse linear relationship between sawdust content and peak bed temperature, with the temperature decreasing by approximately 2.59 °C for every 1% increase in sawdust content ($T_{peak} = 917.93 - 2.593 \times S$, $R^2 = 0.9943$). This strong correlation indicates that sawdust content was the dominant factor governing the observed variation in peak bed temperature within the investigated range. The trend is consistent with the higher calorific value and fixed-carbon content of coal compared with sawdust. As the coal fraction increased, more thermal energy was released within the fuel bed, resulting in higher combustion temperatures. Heat transfer and heat losses also influenced the temperature distribution, as heat was transported by combustion gases, lost through reactor walls, and consumed by devolatilization and gasification reactions.

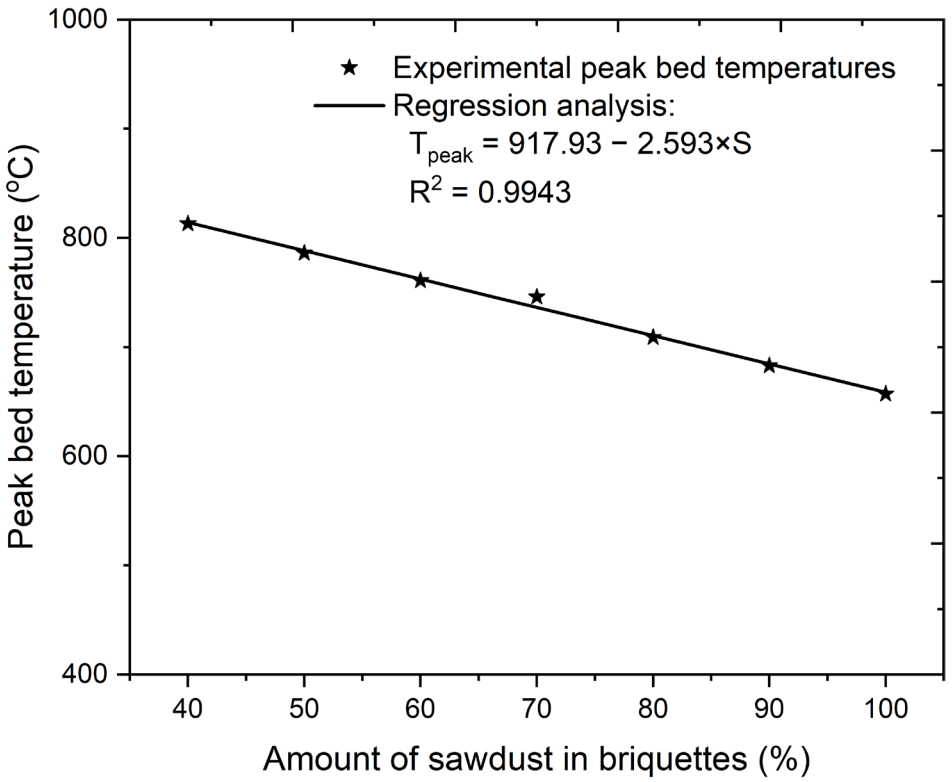


Figure 5. Peak bed temperatures for briquettes made with different compositions of coal and sawdust; S represents sawdust content (%).

Combustion duration exhibited the opposite trend. Pure sawdust briquettes burned for approximately 21 min, whereas briquettes containing 40% sawdust burned for about 26 min. Since all briquettes were combusted under identical operating conditions, the observed differences are primarily associated with fuel composition and its influence on fuel conversion. The shorter combustion duration of sawdust-rich briquettes may also be associated with differences in briquette structure and fuel reactivity, as variations in particle

packing and internal transport characteristics can influence heat and oxygen transfer within the bed [18,19]. These structural effects are considered possible contributing factors to the observed combustion behavior rather than definitive mechanisms.

3.2. Mass-Loss History

The influence of fuel composition on the fuel-conversion is illustrated by the normalized mass-loss histories in Figure 6. Mass decreased continuously during combustion due to moisture evaporation, devolatilization, and oxidation, with gasification potentially contributing to fuel conversion. The slope of each curve represents the rate of mass loss, with steeper slopes indicating faster mass reduction. Pure sawdust briquettes generally exhibited faster mass loss than coal-rich briquettes, possibly due to the higher volatile matter content and greater ease of thermal decomposition of biomass.

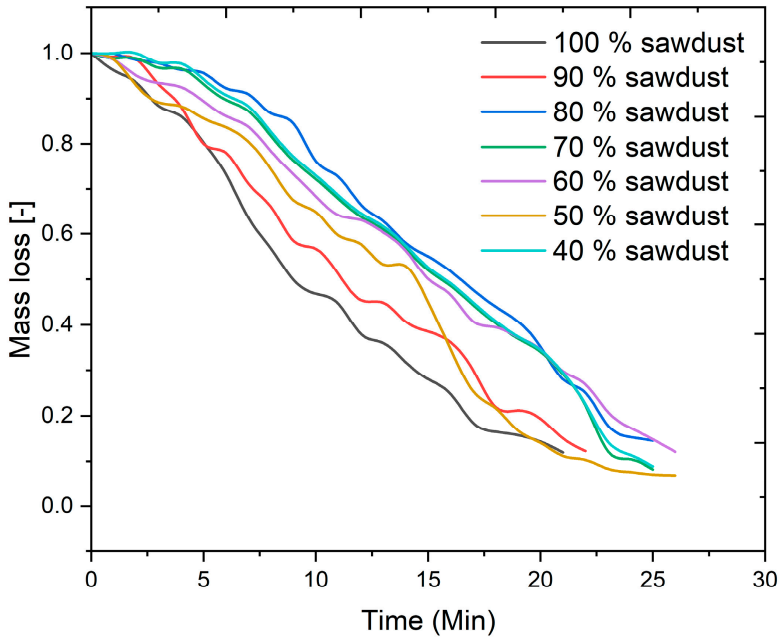


Figure 6. Normalized mass loss history for briquettes made with different compositions of coal and sawdust.

Although mass-loss rates generally increased with sawdust content, the trend was less consistent for formulations containing below 80 wt.% sawdust. This contrasts with Figure 5, where peak bed temperature decreased from approximately 810 °C at 40 wt.% sawdust to 655 °C at 100 wt.% sawdust. The difference may arise because peak temperature reflects the net balance between heat released during oxidation, energy consumed by fuel heating and moisture evaporation, and heat transfer to the surroundings, whereas mass-loss behavior depends on the combined effects of moisture removal, devolatilization, volatile combustion, char oxidation, and heat and mass transfer. These processes may respond differently to changes in fuel composition, resulting in distinct trends in temperature and mass loss.

Furthermore, the fixed air mass flux of 0.10 kg m^{-2} s^{-1} provided a common operating condition but did not guarantee equivalent oxygen availability, as the different blends may have different theoretical oxygen requirements. This may have contributed to the variations in mass-loss behavior. Overall, increasing the sawdust content generally promoted faster fuel conversion, consistent with the shorter combustion durations observed in Section 3.1, although the response was not uniform across all compositions. Further experiments at different air mass fluxes may help clarify the combined effects of fuel composition and oxygen supply on combustion behavior.

3.3. Ignition Characteristics

Ignition times for the different sawdust–coal briquette compositions are presented in Figure 7. Ignition time generally decreased with increasing sawdust content, from approximately 330 s for the 40% sawdust–60% coal briquettes to about 235 s for the 100% sawdust briquettes. Regression analysis confirmed a strong inverse relationship between sawdust content and ignition time, with ignition time decreasing by approximately 1.31 s for every 1% increase in sawdust content ($t_{ign} = 365.544 - 1.312 \times S$, $R^2 = 0.9062$). Thus, under the conditions investigated, coal-rich briquettes required a longer heating period before sustained combustion was established.

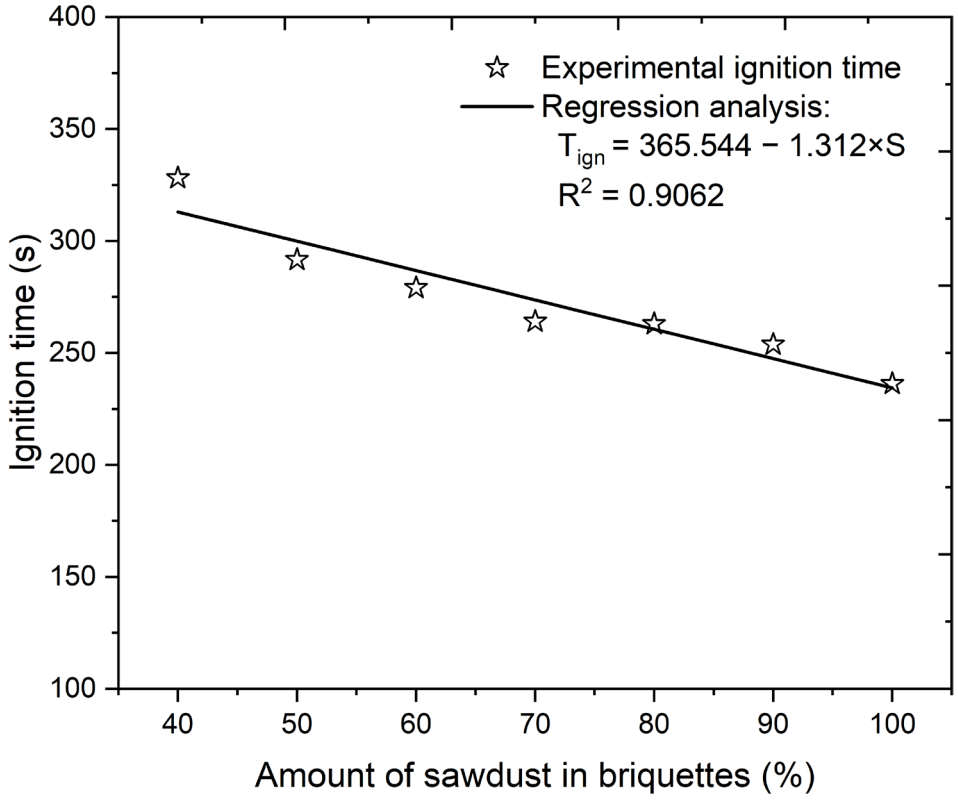


Figure 7. Ignition times for briquettes made with different compositions of coal and sawdust; S represents sawdust content (%).

The observed variation may be associated with differences in fuel composition and the resulting combustion behavior. Although fuel characteristics, particle size, heating conditions, and gas flow may influence ignition, their individual effects were not isolated in this study. Since briquette dimensions and operating conditions were kept consistent while composition was varied, the observed differences in ignition time are primarily associated with the change in fuel composition, while acknowledging that other interacting factors may also contribute.

The proximate analysis (Table 1) shows that sawdust contained substantially more volatile matter (81.02%) than coal (54.81%), which may have promoted earlier release of combustible volatiles and contributed to the shorter ignition times of sawdust-rich briquettes. In contrast, the higher calorific value of coal (20.80 MJ/kg compared with 16.61 MJ/kg for sawdust) implies that more heat may be required to raise coal-rich briquettes to the conditions necessary for sustained combustion, potentially contributing to their longer ignition delay. Changes in sawdust–coal composition may also have altered particle packing and internal transport characteristics, potentially affecting heat and mass transfer during ignition. Overall, the results indicate that increasing sawdust content was associated

with earlier establishment of sustained combustion, whereas increasing coal content was associated with a longer ignition period.

3.4. Flame Propagation Behavior

Following ignition, the combustion front propagated through the fuel bed at different rates, as shown in Figure 8. The average flame propagation speed increased progressively with increasing sawdust content, from approximately 0.132 mm s^{-1} at 40% sawdust to 0.173 mm s^{-1} at 100% sawdust, corresponding to an increase of approximately 31%. Regression analysis confirmed a strong positive linear relationship between sawdust content and flame propagation speed, which is described by $V_f = 0.10246 + 0.0007362 \times S$ ($R^2 = 0.9773$). Thus, within the investigated composition range, increasing the sawdust content was associated with a progressively faster advance of the combustion front. The measured propagation speeds fall within the range of 0.05–0.30 mm s^{-1} that has been reported for biomass combustion in fixed-bed reactors [21,28].

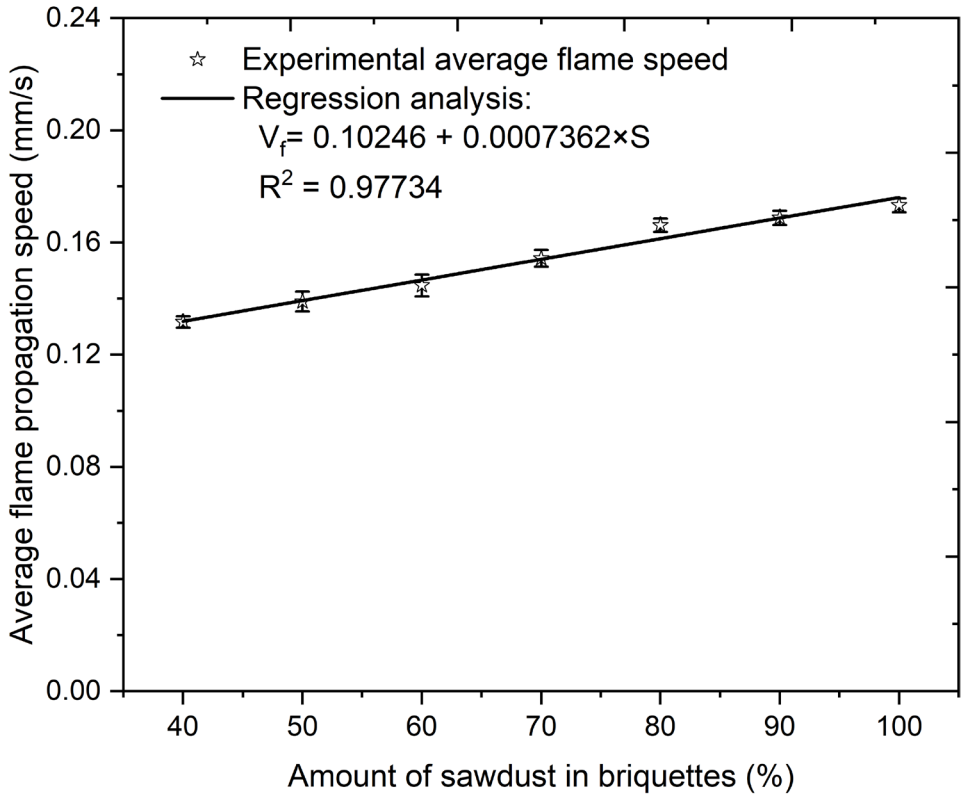


Figure 8. Flame propagation speed for briquettes made with different compositions of coal and sawdust.

The increase in flame propagation speed with increasing sawdust content may be associated with differences in fuel composition and combustion behavior. The higher volatile matter content typically associated with biomass can promote rapid release and combustion of volatile species, facilitating heat transfer to adjacent unreacted fuel and accelerating combustion-front advancement. Conversely, the higher coal fraction may require greater heat input for devolatilization and subsequent char oxidation, potentially reducing the heat available for preheating and igniting successive regions of the bed. Differences in particle packing and internal heat and mass transfer characteristics may also influence flame-front propagation [19,22]. These factors may collectively explain the observed increase in propagation speed with sawdust content and are consistent with the higher mass-loss rates observed for sawdust-rich briquettes (Figure 6).

The error bars represent the standard deviation of propagation speeds across the three thermocouple segments within each combustion run. They therefore represent segment-to-segment variability within a run rather than uncertainty associated with independent experimental replicates.

3.5. Burning Rate Characteristics

The combined effects of fuel conversion and flame propagation are reflected in the burning rates shown in Figure 9. Overall, the burning rate increased with increasing sawdust proportion, although the trend was not monotonic at intermediate compositions. The burning rate increased from 13.99 kg/m^{2}h at 40% sawdust to 17.72 kg/m^{2}h at 100% sawdust, representing an overall increase of 26.7%. At intermediate compositions, the rate increased from 13.99 kg/m^{2}h at 40% to 15.40 kg/m^{2}h at 50%, decreased to 14.10 kg/m^{2}h at 60%, and subsequently fluctuated between 14.18 and 15.42 kg/m^{2}h for sawdust proportions of 70–90%.

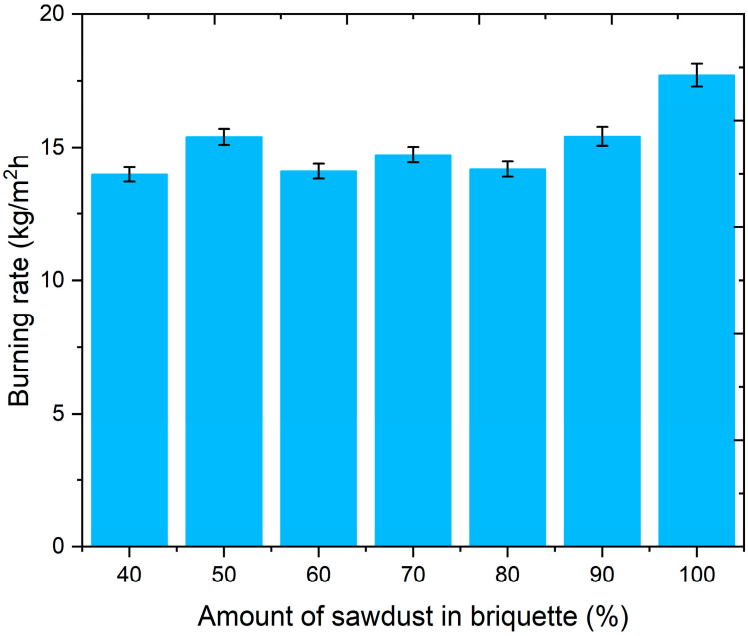


Figure 9. Burning rates for briquettes made with different compositions of coal and sawdust.

The error bars represent the propagated uncertainty associated with mass loss, reactor cross-sectional area, and burning time. The uncertainty in the burning rate was estimated using the law of propagation of uncertainty based on a first-order Taylor series expansion as shown in Equation (3) [29,30].

$$\frac{u(BR)}{BR} = \sqrt{\left(\frac{u(\Delta m)}{\Delta m}\right)^2 + \left(\frac{u(A)}{A}\right)^2 + \left(\frac{u(t)}{t}\right)^2} \quad (3)$$

where BR is the burning rate, Δm is the mass loss, A is the reactor cross-sectional area, t is the burning time, and $u(\Delta m)$, $u(A)$, and $u(t)$ are the corresponding standard uncertainties associated with mass loss, reactor cross-sectional area, and burning time, respectively.

The higher burning rates of sawdust-rich briquettes are consistent with the higher mass-loss rates (Figure 6) and generally higher flame propagation speeds (Figure 8). The greater volatile matter content of sawdust likely promotes fuel devolatilization and combustion, resulting in enhanced fuel conversion [12,13]. However, the non-monotonic trend indicates that volatile matter alone does not govern the burning rate. Variations in briquette structure, porosity, internal heat and mass transfer may also influence combustion behavior.

Although coal-rich briquettes achieved higher combustion temperatures (Figure 5), the maximum burning rate occurred for the 100% sawdust briquette, demonstrating that peak temperature alone is not a sufficient predictor of fuel consumption. Overall, the burning-rate behavior reflects the combined influence of fuel composition, volatile matter content, flame propagation, and internal transport processes within the briquette [31].

The results collectively demonstrate that fuel composition strongly influences the combustion characteristics of sawdust-coal briquettes. Increasing the coal content enhanced the peak bed temperature and prolonged the combustion duration, reflecting the higher calorific value and fixed-carbon content of coal. In contrast, increasing the sawdust content reduced the ignition time and enhanced the mass-loss rate, flame propagation speed, and burning rate, indicating more rapid fuel conversion and combustion-front advancement. These effects may be associated with the higher volatile matter content, greater fuel reactivity, and improved internal transport characteristics of sawdust-rich briquettes. Consequently, coal-rich briquettes produced hotter and longer-lasting combustion, whereas sawdust-rich briquettes promoted earlier ignition, faster flame propagation, and higher fuel-conversion rates. Overall, the results suggest that the optimum briquette composition should balance thermal output and combustion reactivity according to the intended application.

4. Conclusions

This study investigated the influence of fuel composition on the combustion characteristics of sawdust-coal briquettes in a fixed-bed combustor. All briquette formulations exhibited a single dominant temperature peak, suggesting substantial overlap of fuel heating, devolatilization, volatile combustion, and char oxidation processes. Peak bed temperature decreased from approximately 813 °C for briquettes containing 40% sawdust to 657 °C for pure sawdust briquettes, reflecting the higher calorific value and fixed-carbon content of coal. Similarly, combustion duration decreased with increasing sawdust content, indicating more rapid fuel conversion in sawdust-rich briquettes.

The mass-loss rate generally increased with increasing sawdust proportion, demonstrating enhanced fuel conversion. Ignition time decreased from approximately 330 s to 235 s as sawdust content increased, while flame propagation speed increased significantly from 0.132 to 0.173 mm/s. The burning rate also increased with sawdust content, although the trend was not strictly monotonic at intermediate compositions.

Overall, briquette composition strongly influenced the measured combustion characteristics under a fixed air mass flux of 0.10 kg/m^{2}s. Increasing the coal content was associated with higher peak temperatures and longer combustion durations, whereas increasing the sawdust content promoted earlier ignition, faster flame propagation, higher mass-loss rates, and greater burning rates. These contrasting trends demonstrate that combustion intensity, as represented by peak temperature, is not necessarily equivalent to fuel-conversion rate. The results should be interpreted within the context of the fixed air-supply condition, since different fuel blends may have different oxygen requirements. Consequently, peak temperature and burning rate should be considered complementary rather than interchangeable indicators of combustion performance. The findings provide a basis for selecting sawdust-coal blending ratios according to the desired balance between thermal output and combustion reactivity in fixed-bed combustion systems.

Author Contributions: Conceptualization, J.M.N., S.M.N. and Z.H.; methodology, J.M.N., S.M.N. and Z.H.; software, J.M.N.; validation, J.M.N., S.M.N. and Z.H.; formal analysis, J.M.N. and S.M.N.; investigation, J.M.N., S.M.N. and Z.H.; resources, Z.H.; data curation, J.M.N. and S.M.N.; writing—original draft preparation, J.M.N.; writing—review and editing, J.M.N., S.M.N. and Z.H.; visualization, S.M.N.; supervision, Z.H.; project administration, J.M.N. and Z.H.; funding acquisition, Z.H. All authors have read and agreed to the published version of the manuscript.

Funding: This research received no external funding.

Data Availability Statement: The data that supports the findings of this study are available from the corresponding author upon request.

Acknowledgments: The authors would like to acknowledge Tshwane University of Technology for providing the materials, technical support, and facilities that contributed to the successful completion of this research.

Conflicts of Interest: The authors declare no conflicts of interest.

Abbreviations

The following abbreviations are used in this manuscript:

ADC	Analogue-to-Digital Converter
CO_2	Carbon Dioxide
HHV	Higher Heating Value
NO_x	Nitrogen Oxides
PAHs	Polycyclic Aromatic Hydrocarbons
PM	Particulate matter
SO_X	Sulphur Oxides
TCs	Thermocouples
TGA	Thermogravimetric Analysis

References

1. Dudziec, P.; Stachowicz, P.; Stolarski, M.J. Diversity of Properties of Sawmill Residues Used as Feedstock for Energy Generation. *Renew. Energy* **2023**, *202*, 822–833. [CrossRef]
2. Zhang, Z.; Pang, S. Experimental Investigation of Biomass Devolatilization in Steam Gasification in a Dual Fluidised Bed Gasifier. *Fuel* **2017**, *188*, 628–635. [CrossRef]
3. Elmay, Y.; Jeguirim, M.; Dorge, S.; Trouvé, G.; Said, R. Evaluation of Date Palm Residues Combustion in Fixed Bed Laboratory Reactor: A Comparison with Sawdust Behaviour. *Renew. Energy* **2014**, *62*, 209–215. [CrossRef]
4. Khalid, Y.; Tahir, A.; Akhtar, N.; Khan, I.; Tahir, F.; Arshad, M.; Raza, A. From Waste to Energy: Investigating Sawdust Combustion as a Cleaner Alternative to Coal. *Carbon Neutr. Syst.* **2025**, *1*, 10. [CrossRef]
5. U.S. Energy Information Administration Short-Term Energy Outlook. Available online: https://www.eia.gov/outlooks/steo/pdf/steo_full.pdf (accessed on 26 August 2026).
6. Saletnik, A.; Saletnik, B.; Puchalski, C. Coal as the World's Dominant Energy Source and Its Role in the Energy Transformation and Regulations of European Green Deal. *J. Environ. Manag.* **2025**, *392*, 126815. [CrossRef] [PubMed]
7. Junussov, M.; Zholtayev, G.Z.; Kembayev, M.K.; Umarbekova, Z.T.; Mashrapova, M.A.; Antonenko, A.A.; Fu, B. Coal Research in the Global Energy Transition: Trends and Transformation (1975–2024). *Energies* **2026**, *19*, 1017. [CrossRef]
8. Munyao, C.M.; Kiptoo, K.K.G.; Simiyu, G.M. Assessment of Health Risks Associated with Particulate Matter and Carbon Monoxide Emissions from Biomass Fuels Utilization in Western Kenya. *Eur. J. Health Sci.* **2022**, *7*, 39–57. [CrossRef]
9. Whitehill, A.R.; Long, R.W.; Urbanski, S.P.; Colón, M.; Habel, A.; Landis, M.S. Evaluation of Cairpol and Aeroqual Air Sensors in Biomass Burning Plumes. *Atmosphere* **2022**, *13*, 877. [CrossRef] [PubMed]
10. Sabalo, M.J.B.; Villanueva, B.P.; Choi, A.E.S. Research Advances in Selective Catalytic Reduction for Coal Fired Plants. *Environ. Chall.* **2026**, *24*, 101608. [CrossRef]
11. Munawer, M.E. Human Health and Environmental Impacts of Coal Combustion and Post-Combustion Wastes. *J. Sustain. Min.* **2018**, *17*, 87–96. [CrossRef]
12. Gil, M.V.; Casal, D.; Pevida, C.; Pis, J.J.; Rubiera, F. Thermal Behaviour and Kinetics of Coal/Biomass Blends during Co-Combustion. *Bioresour. Technol.* **2010**, *101*, 5601–5608. [CrossRef] [PubMed]
13. Park, D.K.; Kim, S.D.; Lee, S.H.; Lee, J.G. Co-Pyrolysis Characteristics of Sawdust and Coal Blend in TGA and a Fixed Bed Reactor. *Bioresour. Technol.* **2010**, *101*, 6151–6156. [CrossRef] [PubMed]
14. Si, F.; Zhang, H.; Feng, X.; Xu, Y.; Zhang, L.; Zhao, L.; Li, L. Thermodynamics and Synergistic Effects on the Co-Combustion of Coal and Biomass Blends. *J. Therm. Anal. Calorim.* **2024**, *149*, 7749–7761. [CrossRef]
15. Zhai, M.; Tian, X.; Liu, Z.; Zhao, Y.; Deng, Y.; Yang, W. Advancing Just Transition: The Role of Biomass Co-Firing in Emission Reductions and Employment for Coal Regions. *Sustain. Energy Technol. Assess.* **2025**, *75*, 104246. [CrossRef]
16. Bhoi, P.R.; Sarkar, S. The Co-Firing of Pine Biomass and Waste Coal in 100 and 600 MW Power Plants: A Sustainable Approach to Reduce GHG Emissions. *Sustainability* **2025**, *17*, 4473. [CrossRef]

17. Laougé, Z.B.; Merdun, H. Investigation of Thermal Behavior of Pine Sawdust and Coal during Co-Pyrolysis and Co-Combustion. *Energy* **2021**, *231*, 120895. [CrossRef]
18. Mahapatra, S.; Dasappa, S. Experiments and Analysis of Propagation Front under Gasification Regimes in a Packed Bed. *Fuel Process. Technol.* **2014**, *121*, 83–90. [CrossRef]
19. Porteiro, J.; Patiño, D.; Moran, J.; Granada, E. Study of a Fixed-Bed Biomass Combustor: Influential Parameters on Ignition Front Propagation Using Parametric Analysis. *Energy Fuels* **2010**, *24*, 3890–3897. [CrossRef]
20. Kipngetich, P.; Kiplimo, R.; Tanui, J.K.; Chisale, P.C. Optimization of Combustion Parameters of Carbonized Rice Husk Briquettes in a Fixed Bed Using RSM Technique. *Renew. Energy* **2022**, *198*, 61–74. [CrossRef]
21. Tanui, J.K.; Kioni, P.N.; Mirre, T.; Nowitzki, M. The Effect of Carbon Dioxide on Flame Propagation Speed of Wood Combustion in a Fixed Bed under Oxy-Fuel Conditions. *Fuel Process. Technol.* **2018**, *179*, 285–295. [CrossRef]
22. Tanui, J.K.; Kioni, P.N.; Mirre, T.; Nowitzki, M.; Karuri, N.W. The Influence of Particle Packing Density on Wood Combustion in a Fixed Bed under Oxy-Fuel Conditions. *Energy* **2020**, *194*, 116863. [CrossRef]
23. Kipngetich, P.; Kiplimo, R.; Tanui, J.K.; Chisale, P. Effects of Carbonization on the Combustion of Rice Husks Briquettes in a Fixed Bed. *Clean. Eng. Technol.* **2023**, *13*, 100608. [CrossRef]
24. Lienhard, J.H.; Lienhard, J.H. *A Heat Transfer Textbook*, 3rd ed.; Phlogiston Press: Cambridge, MA, USA, 2008.
25. Rohsenow, W.M.; Hartnett, J.P.; Cho, Y.I. (Eds.) Handbook of Heat Transfer. In *McGraw-Hill Handbooks*, 3rd ed.; McGraw-Hill Education LLC: Chicago, IL, USA, 1998.
26. Khor, A.; Ryu, C.; Yang, Y.; Sharifi, V.N.; Swithenbank, J. Straw Combustion in a Fixed Bed Combustor. *Fuel* **2007**, *86*, 152–160. [CrossRef]
27. Yang, Y.; Ryu, C.; Khor, A.; Yates, N.; Sharifi, V.; Swithenbank, J. Effect of Fuel Properties on Biomass Combustion. Part II. Modelling Approach—Identification of the Controlling Factors. *Fuel* **2005**, *84*, 2116–2130. [CrossRef]
28. Dasappa, S.; Paul, P.J. Gasification of Char Particles in Packed Beds: Analysis and Results. *Int. J. Energy Res.* **2001**, *25*, 1053–1072. [CrossRef]
29. Taylor, B.N. *Guidelines for Evaluating and Expressing the Uncertainty of NIST Measurement Results*; NIST Technical Note 1297, 1994 ed; National Institute of Standards and Technology: Gaithersburg, MD, USA, 1994.
30. Taylor, J.R. *An Introduction to Error Analysis: The Study of Uncertainties in Physical Measurements*, 2nd ed.; University Science Books: Sausalito, CA, USA, 1997.
31. Ryu, C.; Yang, Y.B.; Khor, A.; Yates, N.E.; Sharifi, V.N.; Swithenbank, J. Effect of Fuel Properties on Biomass Combustion: Part I. Experiments—Fuel Type, Equivalence Ratio and Particle Size. *Fuel* **2006**, *85*, 1039–1046. [CrossRef]

Disclaimer/Publisher's Note: The statements, opinions and data contained in all publications are solely those of the individual author(s) and contributor(s) and not of MDPI and/or the editor(s). MDPI and/or the editor(s) disclaim responsibility for any injury to people or property resulting from any ideas, methods, instructions or products referred to in the content.